P09

Anode Properties of Tin Based Oxides for Sodium-Ion Batteries

Ying-Ching Lu[1], Nikolay Dimov[2], Shigeto Okada[2*]

[1] *Department of Chemical Engineering, Faculty of Engineering, Kyushu University, Fukuoka 819-0395, Japan*

[2] *Institute for Materials Chemistry and Engineering, Kyushu University, Fukuoka 816-8580, Japan*

**Corresponding author: s-okada@cm.kyushu-u.ac.jp*

Abstract

Herein we report the synthesis and the electrochemical properties of tin oxide-based anodes for sodium-ion batteries: SnO, SnO_2, and SnO_2/C. These oxides react reversibly with Na ion. SnO exhibits the highest reversible capacity and the best cycle life. The data suggest that Sn-based oxide anodes, SnO in particular, could be viable high-capacity anodes for sodium-ion batteries.

1. Introduction

Because of their high energy density, lithium-ion batteries (LIB) have attracted a great deal of attention for large-scale applications beyond their traditional use in portable electronics. However, high material cost hinders the wide commercialization for large-scale applications. For this reason, sodium-ion batteries (SIB) are being considered as possible minor metal-free drop-down replacements for their lithium-ion counterparts. However, many of the anodes used in lithium-ion batteries such as graphite or silicon are electrochemically inactive towards sodium. On the other hand, Na can alloying with few elements [1], those alloy anodes show higher capacity than carbon-base material. Among those alloy anodes, Sn, and Sn-based materials are considered as a possible high-capacity anodes for SIB. However, the poor cyclability owing to the large volume expansion is well known and has been studied in the LIB field. Similarly, tin oxide can be reduced by conversion with Na, generating Sn and further alloying with Na. The Na_2O which forms during conversion reaction can prevent the agglomeration and reduce the volume expansion of tin [2-3]. Therefore, tin oxide could potentially be used as an anode material for Na-ion storage. Here, we investigated the anode performances of tin oxides for sodium-ion batteries through the comparison of the SnO and SnO_2.

2.Experimental

SnO and SnO_2/C anode materials were prepared by hydrothermal method. $SnCl_2 \bullet 2H_2O$ or $SnCl_4 \bullet 5H_2O$ were dissolved in 0.25M citric acid and 0.1M sucrose solution. Then, ~20% aqueous ammonia solution was added drop wise to adjust the solution to pH 10. Afterwards these tin precursor solutions were transferred to Teflon flasks and treated at 150°C and 180°C for 8h. Finally, SnO_2/C materials were carbonized at 550°C for 1h in Ar, and SnO_2 without carbon were synthetized in the same procedure without sucrose.

Electrochemical measurements were carried out in two electrode coin cells. Working electrode consisted of 70 wt% active material, 20 wt% acetylene black (AB) and 10 wt% Carboxymethyl Cellulose (CMC). Sodium metal foil was used as a counter electrode. Charge-discharge measurements were performed under constant current density 50 mA/g in the voltage range 5 mV - 2.0 V.

3. Chapter Title

Figure 1 shows XRD patterns of SnO and SnO_2/C

powders. Voltage profiles and cycle performance of SnO, SnO_2/C electrodes are shown in Fig.2 and Fig.3. In Fig.3 both SnO and SnO_2/C shows higher capacity than SnO_2. The Reversible capacity of our SnO and SnO_2/C electrodes in the first cycle are 440, 412 mAh/g, respectively. The irreversible capacity in the first cycle of SnO and SnO_2/C are 38% and 49%. First cycle irreversible capacity can be attributed to the nature of the conversion reaction, irreversibly consuming Na^+ during the initial cycle, as well as the decomposition of electrolyte and the formation of solid electrolyte interface (SEI). These data show that tin oxides, especially SnO, can provide viable anodes with large capacity for sodium-ion batteries. TEM images of the SnO and SnO_2/C electrodes under various states of charge are shown in Figure 3. Initial discharging of both SnO and SnO_2/C confirms the nature of the conversion reaction with detectable end products Sn and Na_2O (Fig 3 (e), (f)). All observed diffraction rings belong to either Sn or Na_2O. However, the distribution of the Sn nanoparticles within the Na_2O matrix of the converted SnO_2/C electrode is uniform with average Sn particle size around 2-5nm (Fig 3 (b), (d)). In contrast, the Sn nano-particles that formed in the converted SnO electrode show random particle size distribution and the density of Sn within the Na_2O matrix is higher as expected owing to the higher Sn:O atomic ratio in SnO than in SnO_2. After the first charging to 2.0V, the particles grew in both electrodes as shown in Figure 4. SAED patterns (Fig 4 (e), (f)) reveals that charging results in particles with reduced crystallinity. They can be indexed as SnO_2 and Sn. After charging the converted SnO electrode to 2V, its constituents Sn and Na_2O did not reverse back to the pristine SnO because SnO_2 is the only thermodynamically stable phase.

4. Conclusion

SnO, SnO_2, and SnO_2/C samples were prepared by hydrothermal reactions and explored as anode materials for SIB. A uniform SnO_2/C nanoparticle sample was obtained in the presence of glucose. SnO_2/C showed better capacity and better capacity retention compared with the bare SnO_2. Despite large, uneven particle size, and particle size distribution, SnO outperformed both SnO_2 and SnO_2/C. Demonstrating high reversible capacity, low polarization, and low irreversible capacity loss. SnO is the only sample in the studied series that did not show capacity loss for at least 50 cycles, and Sn utilization increased over cycles.

Acknowledgment

This work was financially supported by the Elements Science & Technology Projects of MEXT, Japan.

Reference

[1] L. Xiao, Y. Cao, J. Xiao, W. Wang, L. Kovarik, Z. Niea, J. Liu, *Chem. Commun.*, **48**, (2012) 3321..

[2] D. Su, H.J. Ahn, G. Wang, *Chem. Commun.*, **49**, (2013) 3131.

[3] 12. D. Su, C. Wang, H. Ahn, G. Wang, *Phys. Chem. Chem. Phys.*, **15**, (2013) 12543.

Email: 3ES12018N@s.kyushu-u.ac.jp

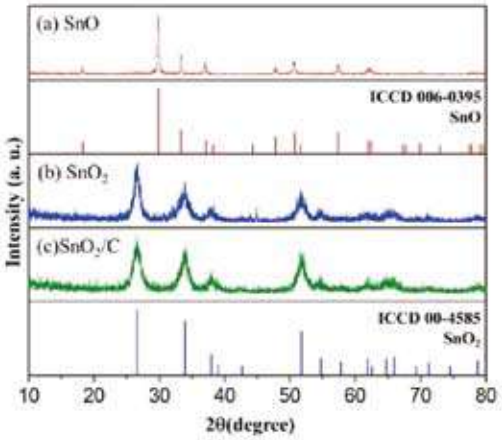

Figure 1. XRD patterns of: (a) SnO, (b) SnO2, and (c) SnO2/C.

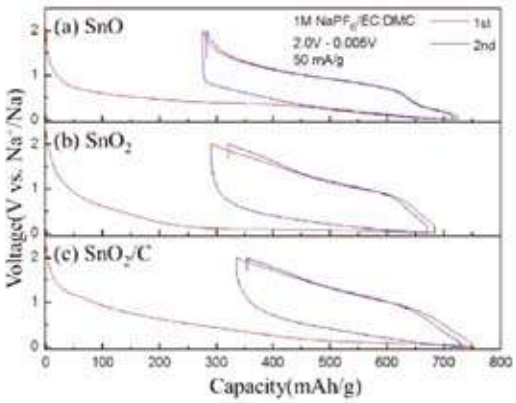

Figure 2. Charge/discharge profiles of: (a) SnO, (b) SnO2, and (c) SnO2/C.

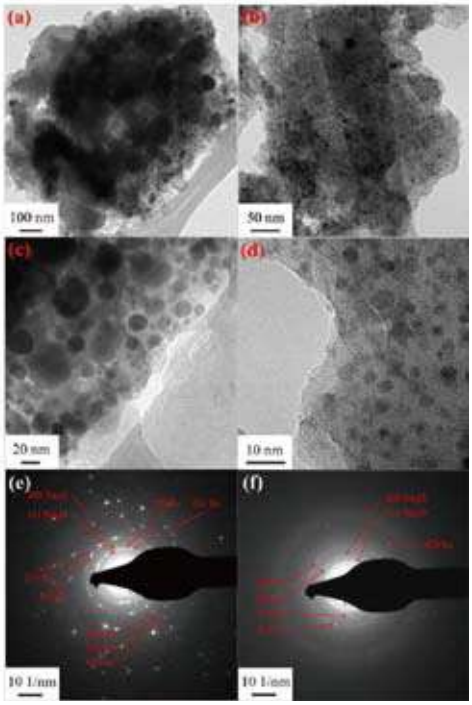

Figure 3. TEM images of (a), (c) SnO (b), (d) SnO_2/C discharge to 5mV and SAED pattern of (e) SnO (f) SnO_2/C discharge to 5mV.

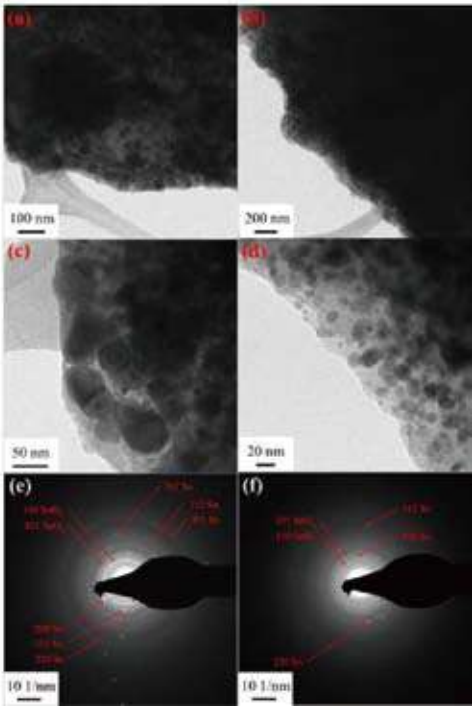

Figure 4. TEM images of (a), (c) SnO (b), (d) SnO_2/C charge to 2V and SAED pattern of (e) SnO (f) SnO_2/C charge to 2V.